RESEARCH ARTICLE

Localization of the bioadhesive precursors of the sandcastle worm, *Phragmatopoma californica* (Fewkes)

Ching Shuen Wang and Russell J. Stewart*

Department of Bioengineering, University of Utah, Salt Lake City, UT 84112, USA

*Author for correspondence (rstewart@eng.utah.edu)

SUMMARY

The marine sandcastle worm bonds mineral particles together into underwater composite dwellings with a proteinaceous glue. The products of at least four distinct secretory cell types are co-secreted from the building organ to form the glue. Prominent hetereogeneous granules contain dense sub-granules of Mg and the (polyphospho)proteins Pc3A and B, as well as at least two polybasic proteins, Pc1 and Pc4, as revealed by immunolabeling with specific antibodies against synthetic peptides. Equally prominent homogeneous granules comprise at least two polybasic proteins, Pc2 and Pc5, localized by immunolabeling with anti-synthetic peptide antibodies. The components of the sub-micrometer granule types are unknown, though positive staining with a redox-sensitive dye suggests the contents include *o*-dihydroxy-phenylalanine (dopa). Quantitative PCR and *in situ* hybridization demonstrated that a tyrosinase-like enzyme with a signal peptide was highly expressed in both the heterogeneous and homogeneous granules. The contents of the granules are poorly mixed in the secreted mixture that forms the glue. Subsequent covalent cross-linking of the glue may be catalyzed by the co-secreted tyrosinase. The first three parapodia of the sandcastle worm also contain at least two distinct secretory tissues. The Pc4 protein was immunolocalized to the anterior secretory cells and the tryosinase-like gene was expressed in the posterior secretory cells, which suggests these proteins may have multiple roles.

Supplementary material available online at http://jeb.biologists.org/cgi/content/full/215/2/351/DC1

Key words: bioadhesive, polyelectrolytes, sandcastle worm, *Phragmatopoma californica*, polychaeta, sabellariidae, tyrosinase, dopa, quinonic cross-linking.

INTRODUCTION

Marine polychaetes in the family Sabellariidae live in tubular shells cobbled together with sandgrains, the broken skeletons of marine invertebrates and a protein-based underwater glue. Juvenile worms build new tubes adjoining existing tubes of the same species to create reef-like intertidal and subtidal colonies. *Phragmatopoma californica* (Fewkes), known commonly as the sandcastle worm, is found along the west coast of the USA. The description of a *P. californica* colony from the original classification by Fewkes (Fewkes, 1889) provides a sense of the turbulent habitats preferentially inhabited by sabellariids. To paraphrase, the 'aggregation' was a continuous mass, several feet across and 1–2 feet thick, encrusted onto the roof of a cavern carved by the sea into soft rock cliffs near Santa Barbara, CA, USA. The colony was exposed for several hours between tides. Colonization of high-energy shoreside environments, such as that described by Fewkes, requires robust construction of the honeycomb-like colonies, which reflects the durability of the waterproof adhesive bonds holding the composite tubes together. These qualities have sparked interest in the sandcastle worm glue (Shao et al., 2009), as well as in other marine bioadhesives, notably the byssal adhesive plaques of mytilid mussels (Waite et al., 2005), as sources of natural materials and design principles for underwater adhesives. The potential applications of these bioinspired synthetic adhesives include the repair of wet living tissues (Winslow et al., 2010; Lee et al., 2011).

During tube construction, the sandcastle worm applies miniscule spots of glue to millimeter-sized mineral particles as they are pressed onto the end of the tube. The initially fluid glue sets into a solid foam within 30s of secretion into seawater (Stevens et al., 2007). Jensen and Morse (Jensen and Morse, 1988) discovered that the protein glue contains *o*-dihydroxy-L-phenylalanine (dopa) – post-translationally hydroxylated tyrosine – previously identified in the adhesive plaque proteins of mytilid mussels. The authors also noted the similarities in amino acid composition to the underwater adhesive silk of caddisfly larvae (Trichoptera), in particular the presence of high molar ratios of glycine, serine and basic residues. The chemical similarities have since been shown to go further; the serines in both adhesives are extensively phosphorylated. In total, the sandcastle worm glue and caddisfly silk contain more than 26mol% and nearly 10mol% phosphoserine, respectively (Stewart et al., 2004; Stewart and Wang, 2010). Extensive serine phosphorylation and high proportions of basic residues, especially arginine, are common in aquatic adhesives (Flammang et al., 2009; Stewart et al., 2011). As another example, the giant salivary secretory proteins of midge fly larvae (Diptera), which are drawn as insoluble fibers that are used in the construction of underwater filter feeding webs and pupal cases, contain 25mol% basic residues and 8mol% phosphoserines (Galler et al., 1984; Case et al., 1994). Intermolecular charge neutralization through electrostatic association of oppositely charged regions of polyelectrolytic proteins, with consequent expulsion of water and small counter-ions, may be part of a common mechanism that drives the initial insolubilization of these highly phosphorylated underwater bioadhesives (Case et al., 1994; Stewart et al., 2004; Stewart and Wang, 2010).

Taking into account serine phosphorylation, nearly 50% of the amino acids in the sandcastle worm glue are charged. The first putative glue proteins, Pc1 and Pc2, were isolated from homogenates of the adhesive gland-containing parathorax and sequenced by automated Edman degradation (Waite et al., 1992). Both are highly repetitive, glycine rich, and contain 27 and 34 mol% amine side-chains, respectively. Genes encoding a set of serine-rich proteins, Pc3A and Pc3B, were cloned with oligo serine-encoding PCR primers from a parathorax cDNA library (Zhao et al., 2005). Pc3B is a polyacid consisting entirely of runs of 6–12 phosphoserines punctuated with single tyrosine residues. In contrast, Pc3A is a polyampholytic diblock protein: the N-terminal block contains runs of 4–6 phosphoserines interrupted with single tyrosine residues; the C-terminal block, of roughly equal length, is strongly basic (predicted pI 11.8) comprising 26 and 12 mol% arginine and lysine residues, respectively. The C-terminal domain also contains 10 mol% cysteine residues. The primary structure of Pc3A highlights another striking similarity between the sandcastle worm glue and caddisfly silk proteins – phosphoserine-rich motifs alternate with arginine-rich motifs in both cases. The caddisfly silk heavy chain fibroin protein has short phosphoserine $(pSX)_4$ blocks flanked by short arginine-rich blocks, creating a larger motif that repeats hundreds of times (Yonemura et al., 2006; Stewart and Wang, 2010). In addition to Pc1, Pc2 and Pc3AB, an additional 14 genes encoding proteins with characteristics of structural glue proteins – secretion signal peptides, low complexity sequences and highly repetitive primary structures – were identified by sequencing random clones from a parathorax cDNA library. Most are basic, though some may be ampholytic (Endrizzi and Stewart, 2009).

The sandcastle worm glue originates in a prominent adhesive gland situated around the coelomic cavity of the first three parathoracic segments. The gland consists of multiple cell types, each producing distinct types of secretory granules. The largest and most abundant secretory cell types, present in roughly equal proportions, are densely packed with either 'homogeneous' or 'heterogeneous' granules, both 2–3 μm in diameter (Vovelle, 1965). The contents of the homogeneous granules appear to be of uniform ultrastructure, while the heterogeneous granules contain multiple sub-granules of widely varying diameter. Elemental analysis by energy dispersive x-ray spectroscopy revealed P and Mg concentrated exclusively in the sub-granules of the heterogeneous granules, undoubtedly in the form of Mg^{2+} complexed with phosphorylated Pc3 (Wang et al., 2010). The homogeneous and heterogeneous granules travel, intact, through narrow extensions leading from their respective secretory cell bodies to the periphery of the building organ, some from as far away as the posterior boundary of the third segment. At least two other types of much smaller, sub-micrometer secretory granules originate in cells situated around the base of the building organ. Only after the granules have exited intact through the building organ surface do their contents mix and become a viscous adhesive foam (Wang et al., 2010).

Clearly, the sandcastle worm builds composite mineral structures with a multi-part adhesive, the reactive components of which are separately packaged in condensed granules, though much remains unknown about the natural bioadhesive. Conclusive evidence that Pc1 and Pc2 are components of the primary glue used to bond mineral particles into tubes has not been reported. Because the proteins were isolated from parathorax homogenates it remains possible that they are constituents of the several other secretory cell types that surround the parathorax (Wang et al., 2010). Likewise, the cDNA library in which putative glue protein genes were identified was constructed with parathorax mRNA (Zhao et al.,

2005). Transcripts of proteins actively secreted from other regions of the parathorax would be well represented in the library in addition to the adhesive gland. Better understanding of which components are packaged into which adhesive granules, when and how the separated components are mixed prior to bonding, and the chemical details of the setting and hardening reactions will guide development of more sophisticated next-generation mimetic adhesives (Shao et al., 2009). Toward this goal, the catalog of genes expressed in the adhesive gland (Zhao et al., 2005; Endrizzi and Stewart, 2009) was used to create specific nucleic acid and antibody probes to better understand the molecular organization of the sandcastle worm adhesive system.

MATERIALS AND METHODS
Animal preparation

Phragmatopoma californica colonies were collected near Santa Barbara, CA, USA, and shipped overnight to Salt Lake City, UT, USA. The colonies were maintained in a laboratory aquarium with circulating artificial salt water (Instant Ocean, Spectrum Brands Inc., Madison, WI, USA) chilled to 14°C.

Histochemistry

Worms were carefully removed from their tubes and rinsed with filtered saltwater three times before fixation. Worms were fixed with 4% paraformaldehyde (Polyscience Inc., Warrington, PA, USA) in phosphate-buffered saline (PBS) at 4°C overnight. After fixation, the worms were dehydrated in a series of ethanol solutions (50%, 70%, 95% and 100%), then stored in the freezer or processed immediately. Fixed worms were infiltrated with Immunobed (EM Science, Gibbstown, NJ, USA) according to the manufacturer's instructions. Fully polymerized blocks were serially sectioned (2 μm) on a microtome and mounted on superfrost slides (Fisher Scientific, Pittsburgh, PA, USA). Sections were rehydrated with deionized (DI) water at room temperature (RT) for 5 min, then stained with Toluidine Blue (TB) using standard protocols. Dopa-containing compounds were detected by staining with nitroblue tetrazolium chloride (NBT; $1\,mg\,ml^{-1}$ NBT in $2\,mol\,l^{-1}$ potassium glycinate, pH 9.5) at RT for at least 2 h for color development. Sections were de-stained in $0.16\,mol\,l^{-1}$ sodium borate buffer at RT for 2 h and mounted with a coverslip for light microscopy.

Scanning electron microscopy

Whole worms were fixed in 2% glutaraldehyde with 1% paraformaldehyde in $0.1\,mol\,l^{-1}$ sodium cacodylate buffer at 4°C overnight. Fixed whole worms were dehydrated with serial ethanol and dried with hexamethyldisilazane (HMDS) before scanning electron microscopy (SEM) imaging. To prepare tissue sections, worms were fixed and dehydrated as described above and embedded in Immuno-Bed Resin (Electron Microscopy Science, Hatfield, PA, USA). Worms were sectioned (5 μm) longitudinally, dehydrated with ethanol, and dried with HMDS before SEM imaging.

Sequencing

Random clones from a parathoracic cDNA library were sequenced as described in detail previously (Endrizzi and Stewart, 2009).

Quantitative real-time PCR

RNA was isolated only from worms that rebuilt substantial portions of their tubes with 0.5 mm glass beads within 12 h after the anterior portion of their tubes was removed. Eighteen worms were removed from their tubes and rinsed with filtered seawater three times, then randomly divided into three sets. After the parathorax had been

dissected, total RNA was purified with an RNAeasy kit (Qiagen, Valencia, CA, USA). The amount of RNA from each set was normalized using the ratio of absorbance at 260 and 280 nm. Total RNA was reverse transcribed into cDNA with a SuperScript III first-strand synthesis kit (Invitrogen, Carlsbad, CA, USA). PCR primer sets were designed (supplementary material Table S1) using the Primer3 software analysis tool (Rozen and Skaletsky, 2000). The three separate pools of total cDNA were amplified with gene-specific primers and SYBR mix (Rox, Roche, Indianapolis, IN, USA). Samples were analyzed on a 7900 HT fast real-time PCR system (Applied Biosystems, Concord, MA, USA).

In situ hybridization

Double-stranded DNA templates were amplified by PCR with specific primer sets (supplementary material Table S2). A T7 promoter binding site was added to all reverse strand PCR primers. After PCR amplification, dsDNA templates were isolated with a QIAquick PCR purification kit (Qiagen) and used for RNA probe synthesis. Digoxigenin (DIG)-labeled RNA probes were prepared with T7 RNA polymerase and DIG–dUTP at 37°C for 2 h, then isolated on an RNAeasy mini column (Qiagen). Purified RNA probes were stored in Rnase-free DI water at –80°C until use.

Worms were fixed in 4% paraformaldehyde in DEPC-treated PBS at 4°C overnight. Fixed worms were cryoprotected in freezing medium (Tissue Freezing Medium, EM Science) and cut into 70 μm serial sections on a cryotome. Sections were post-fixed with 4% paraformaldehyde at RT for 15 min. Samples were dehydrated with serial ethanol, followed by rehydration with the reverse serial ethanol solutions. Sections were bleached with 3% H_2O_2 in 0.5% KOH in DEPC-treated de-ionized PBS at RT for 2 h to remove pigmentation for better visualization. Tissue sections were permeabilized with 0.25% Triton X-100/PBS at RT for 20 min, then incubated in pre-hybridization buffer (50% de-ionized formamide, 5× SSC, 1 mg ml^{-1} salmon sperm DNA, 1% Tween-20 and 1% ascorbic acid) at 50°C for 2 h. Before hybridization, RNA probes were denatured at 70°C for 5 min and chilled on ice. Tissue sections with RNA probes were incubated in hybridization buffer (50% de-ionized formamide, 10% dextran sulfate, 5× SSC, 0.5 mg ml^{-1} salmon sperm DNA and 1% Tween-20) at 50°C for 16 h. Post-washing steps were done at 50°C as follows: (1) 2×30 min in 1:1 ratio of pre-hybridization buffer and 2× SSC + 0.1% Triton X-100, (2) 2×30 min 2× SSC + 0.1% Triton X-100, and (3) 2×30 min 0.2× SSC + 0.1% Triton X-100. Sections were returned to RT in PBST (PBS plus 0.05% Triton X-100) for 2×30 min, then blocked with 1% blocking buffer (Blocking reagent, cat. no. 11096176001, Roche) at RT for at least 4 h. Alkaline phosphatase-labeled anti-DIG (1:5000 dilution, cat. no. 11093274910, Roche) was added at 4°C overnight. After washing at least five times with PBST at RT for 30 min each, blue color was developed at RT with NBT/BCIP substrate (Fisher Scientific) in the dark. The signal to background ratio was improved by adding 100% ethanol to the sections for 30 min at RT. Sections were then rehydrated with serial ethanol and mounted on glass slides for imaging. Controls for non-specific antibody binding used anti-DIG as the primary antibody and anti-mouse alkaline phosphatase-conjugated secondary antibody.

Antibodies

Synthetic peptides predicted to be immunogenic (Pc2, residues 133–148, GFNYGANNAIKSTKRF; Pc4, residues 46–60, KKTYRGPYGAGAAK; Pc5, residues 114–128, ALGALGGN-GGFWKRR) were used to generate antibodies in rabbits (Pacific Immunology, Ramona, CA, USA; supplementary material Fig. S1).

Anti-Pc2, anti-Pc4 and anti-Pc5 serum were purified from serum by affinity chromatography with the synthetic peptides coupled to a column (SulfoLink Immobilization Kit, Pierce, Rockford, IL, USA) and stored in PBS with 10% glycerol and 0.05% sodium azide at –20°C until use. Commercial anti-phosphoserine (mouse, ab6639, Abcam, Cambridge, MA, USA) was used to detect highly phosphorylated Pc3 proteins.

Immunostaining

Paraformaldehyde-fixed worms were rehydrated with serial ethanol, frozen in cryoprotectant (Tissue-Tek, Sakura, Torrance, CA, USA) and cryosectioned into 40 μm coronal sections. Sections were bleached with 3% H_2O_2/0.5% KOH in PBS at RT until pigmentation disappeared. Sections were permeabilized with 0.25% Triton X-100 in PBS at RT for 20 min and washed 3×5 min with PBS. Sections were transferred to blocking solution (1% BSA in PBS, 0.1% Triton X-100) at RT for at least 2 h. Blocking solution was replaced with 1:1000 dilution of anti-phosphoserine (Abcam) or the custom-made anti-Pc2, anti-Pc4 and anti-Pc5 antibodies and incubated at 4°C for 12 h. Sections were washed at least 5×15 min in PBST at RT. The sections were then incubated with 1:5000 dilution of either anti-mouse (ab6729, Abcam) or anti-rabbit secondary antibody (ab6722, Abcam) at 4°C for 12 h. Sections were washed at least 5×15 min in PBST at RT. Color was developed with NBT/BCIP substrate (Fisher Scientific) at RT in the dark and monitored carefully under the dissecting microscope. The sections were incubated in 100% ethanol for 30 min at RT to improve the signal to background ratio. Sections were rehydrated with serial ethanol and mounted on glass slides for imaging. Controls for non-specific binding of the mouse anti-phosphoserine antibody used anti-DIG as the primary antibody and alkaline phosphatase (AP)-conjugated, or Alexa 647-conjugated, anti-mouse secondary antibody. Controls for non-specific binding of the rabbit anti-Pc2, anti-4 and anti-5 used pre-immune rabbit serum and AP-conjugated, or Alexa 594-conjugated, anti-rabbit secondary antibody.

Western blots

Secretory granules were isolated by passing parathorax homogenates through a cell strainer (40 μm pore size, BD Biosciences, Sparks, MD, USA). Material passing through the strainer, including homogeneous and heterogeneous secretory granules, was collected in an Eppendorf tube and centrifuged immediately (3000 g for 1 min). Centrifuged pellets were denatured in modified SDS sample buffer (1× SDS sample buffer, 6 mol l^{-1} urea, 0.5 mol l^{-1} DTT), separated by 12% SDS-PAGE, and transferred to PVDF membranes (Fisher Scientific). The membranes were blocked with 1% BSA in PBST solution at RT for 2 h, then incubated with 1:1000 dilution of anti-Pc2, anti-phosphoserine, anti-Pc4 or anti-Pc5 antibody at 4°C overnight. After washing, blots were incubated with anti-mouse (1:5000 dilution, ab6728, Abcam) or anti-rabbit (1:5000 dilution, ab6721, Abcam) secondary antibody at 4°C for 12 h. Incubated film was washed with PBST three times at RT for 5 min then developed with enhanced chemiluminescence substrate (Pierce).

Secreted glue immunostaining

Glass beads bonded by worms to the ends of their tubes were collected with forceps. Glue spots were washed off the glass beads with 30% acetic acid. The glue was collected by centrifugation and mounted in Immuno-Bed resin (Electron Microscopy Science), cut into 5 μm sections and adhered to Superfrost slides (Fisher Scientific). Sectioned glue was dehydrated and rehydrated with serial ethanol solutions at RT for 5 min each then digested with proteinase

K in digestion buffer ($2\,\mu g\,ml^{-1}$ proteinase K in PBS, 0.05% Triton X-100 and 0.1% SDS) at 37°C for 30 min. Samples were blocked with 1% BSA in PBST at RT for 2 h and double-labeled with anti-phosphoserine and anti-Pc2, anti-Pc4 or anti-Pc5 antibody (1:1000 dilution) at 4°C for 12 h. After washing, the sections were incubated with peroxidase-conjugated anti-mouse (1:1000, Alexa647, Invitrogen) or anti-rabbit (1:1000, Alexa594, Invitrogen) secondary antibody at 4°C for 12 h in the dark. Slides were washed with PBST three times at RT for 15 min each and mounted under a coverslip with Prolong anti-fade mounting media (Invitrogen) before imaging. Negative control samples were incubated with anti-DIG (1:1000, mouse, ab420, Abcam) and pre-immune rabbit serum (1:1000, Pacific Immunology) followed by anti-mouse or anti-rabbit secondary antibody. Samples were imaged on a Fluoview FV1000 fluorescent microscope (Olympus) with filter sets (594 and 647 nm) in default settings. Non-specific binding controls were as described earlier. The sandcastle worm glue is weakly autofluorescent. To avoid interference from this autofluorescence, the laser intensity and detector settings were adjusted to levels where the autofluorescence was not visible in unlabeled glue sections. The same laser and detector settings were then used to image the immunolabeled glue sections.

RESULTS

Adhesive gland morphology and secretion pathway

A TB-stained coronal section provides an overview of the adhesive gland system (Fig. 1A). The building organ is the distinct U-shaped structure, within which is the V-shaped mouth. Below the building organ a bowtie-shaped structure is outlined by a layer of distinct cell type. In the main adhesive gland, contained within large secretory cells clustered around the cavity of the first three parathoracic segments, heterogeneous granules were stained dark blue by the cationic dye and homogeneous granules were stained lighter blue. Cellular extensions containing single file heterogeneous or homogeneous granules lead from the major secretory cells to the building organ (Fig. 1D). The granules arrived intact and remained in separate channels around the entire circumference of the building organ (Fig. 1B). At least two additional secretory cell types, differentially stained by TB, were apparent between the base of the building organ and the bowtie (Fig. 1B). The first three, and only the first three, parapodia also stained strongly with TB (Fig. 1A). At higher magnification, multiple types of secretory cells, distinguished by the intensity of staining, were apparent in the anterior and posterior regions of each parapodia (Fig. 1C). The red metachromatic shift at the periphery of the anterior region is characteristic of TB-stained acidic carbohydrates and other acidic biomacromolecules (Bergeron and Singer, 1958). Parapodia posterior to the parathorax did not stain strongly with TB, which suggests the first three parapodia have specialized secretory functions. Nuclei throughout the entire section stain dark blue.

Dopa proteins and other quinonoids, at high pH in the presence of excess glycine, reduce NBT creating a deep blue formazan compound (Paz et al., 1991). Coronal sections of resin-embedded worms were stained with NBT/glycinate to reveal the distribution of dopa proteins in the parathorax. Both homogeneous and heterogeneous granules stained deep blue, outlining the three adhesive gland segments, the bundled channels and the building organ (Fig. 2). The small granules that originate from around the base of the building organ also stained darkly and appeared to be in channels moving toward the surface of the building organ (Fig. 2B). The posterior region of the three parathorax parapodia also stained with NBT (Fig. 2C).

Cells containing sub-micrometer secretory granules were observed by scanning electron microscopy of thin sections through the base of the building organ (Fig. 3A). The small granules were gathered at the edge of the building organ with the much larger heterogeneous and homogeneous granules, all of which emerged from separate channels still intact (Fig. 3B). Addition of dopamine
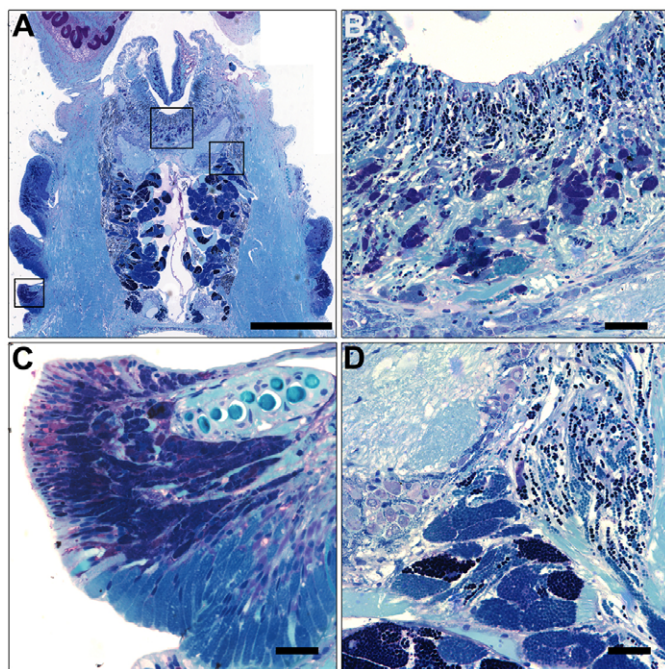

Fig. 1. Coronal section of parathorax stained with TB. (A) Low magnification image of the parathorax. (B) Higher magnification of the region in the top-center box in A. (C) Higher magnification of the parapodia secretory tissues in the region indicated by the bottom-left box in A. (D) Higher magnification of the cellular extensions in the region indicated by top-right box in A. Scale bars: A, 500 μm; B–D, 20 μm.
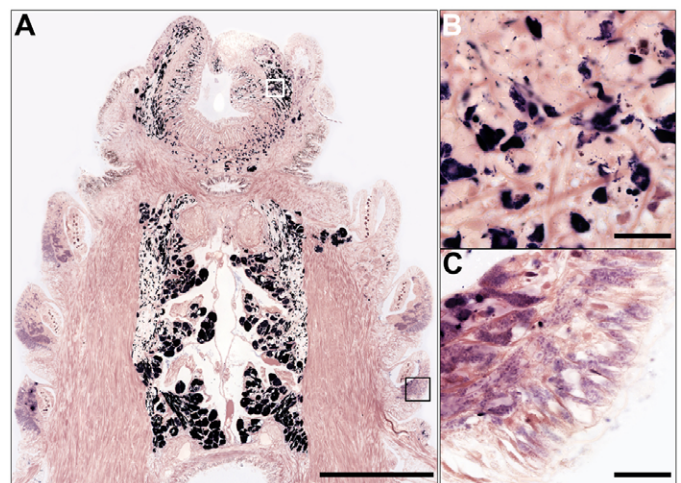

Fig. 2. Nitroblue tetrazolium chloride (NBT) labeling of dopa-containing cells in the parathorax. (A) Coronal cryosection stained with NBT. Redox active groups stain blue. (B) Higher magnification of small secretory granules in the region indicated by the upper box in A. (C) Higher magnification of the parapodia area indicated by the lower box in A. Scale bars: A, 500 μm; B and C, 20 μm.
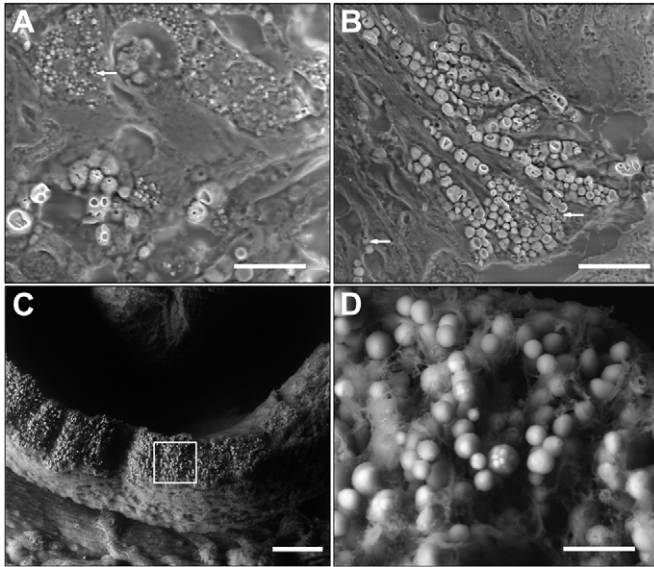
Fig. 3. Scanning electron microscope (SEM) imaging of adhesive precursor granules. (A) SEM image of a thin section through the base of the building organ. The arrow indicates a small granule-producing cell. (B) SEM image of a thin section through the adhesive precursor exit site of the building organ. The arrow indicates small granules in a secretory channel. (C) SEM image of the exterior of the building organ after stimulation of secretion. (D) Higher magnification of the region indicated by the white box in C. Scale bars: A, 10 μm; B, 15 μm; C, 50 μm; D, 5 μm.

to the external seawater caused intact homogeneous and heterogeneous granules to emerge from around the external periphery of the building organ (Fig. 3C,D). The small granules were not apparent and the large granules appeared to be partially embedded in fibrous material.

Expression analysis

Previously, 14 genes encoding proteins with characteristics of secreted structural proteins, a gene encoding a secreted laccase 2, and a gene encoding a cytoplasmic tyrosinase were identified by sequencing clones picked at random from a parathoracic cDNA library (Endrizzi and Stewart, 2009). Additional sequencing of random cDNA clones identified four additional complete open reading frames encoding proteins with characteristics of secreted structural proteins, as well as a second tyrosinase gene (Fig. 4). The new tyrosinase contained a signal peptide, in contrast to the cytoplasmic tyrosinase found earlier, which suggests it is secreted and functions externally.

As a first step in determining their role in the sandcastle worm glue, if any, the expression levels relative to actin of 16 of the putative glue protein genes were estimated by quantitative real-time PCR (Fig. 5). In the laboratory, healthy worms will rebuild damaged portions of their tubes if sand or glass beads are provided as building materials (Jensen and Morse, 1988). For quantitative expression analysis, mRNA was isolated from the parathoracic region only of worms actively rebuilding tubes in the lab to ensure active expression of glue protein genes. The Pc3A and Pc3B PCR primers were designed to amplify all variants of the transcripts (supplementary material Fig. S2). Pc1–5 and tyrosinase 1 had the highest expression levels, with Pc1 expressed at nearly the same level as actin (Fig. 5). Combined, expression of all variants of the polyphosphoserine proteins Pc3A and Pc3B was approximately 40% that of Pc1. Notably, tyrosinase 1 was the fourth most abundant transcript. Expression of all other genes, including the cytoplasmic tyrosinase 2 and laccase 2, was 1% or less than that of Pc1 and therefore they may not play major structural or enzymatic roles in glue formation (supplementary material Tables S3, S4). Further analysis of the low expression genes was not pursued.

In situ hybridization

Tissue and cellular expression sites were located by *in situ* hybridization with DIG-labelled RNA probes from unique regions

---

Pc19   MW 20,466   pI 6.98
MKLSIALVLFAVLVSSING
GGYGDNQGGYGGSIYIGQFTGKCGSDGLYS
MTENSYVSCTHGRAYVLPCAPGTLDRSGAL
CGVNLVDRGYAAVKSVTSVIK
GYGQSSGGHSGGG
GYGSSSGGYSSGGGYGYGSGGHSGGS
GYGSSSGGPSGGGGYGYSSGGHSGGS
GYGSSSGGYSGGSGGGYEYSSGGHIGGS
GYGSSSGGYSGGSSGYGKSGGHEDSG

Pc21   MW 22,347   pI 7.62
MKFFILAACLALVYASGPVKDDDEYKETREYT
KEYTVDRNKGYNRK
GYGDDVSAKETFLRTTEYNDKD
GYGSKNDGKQVKESYTREYEIDKD
GYGKDDDVTGKETYRREVTVDDD
GYSPRGRYGRTDAY
GLNDGYVRKDAY
GLRRGP
GLGVYPGP
GLGRKDVYPATGLGRKDVYPVT
GLGRKDVYPATGLGRKDVYPAT

Pc22   MW 18,631   pI 5.32
MLVSLLLIGLVMIVRSDIHGLV
MEDAPGPSPSTSRVRESRDIHGLV
MEDAPGPSPSTSRVRESRDIHGLV
MEDAPGPSPSTSRVRESRDIHGLV
MEDAPGPSPSTSRVRESRDIHGLV
MEDAPGPSPSTSRVRESRDIHGLV
MEDAPGPSPSTSRVRESRDIHGLV
MEDAPGPS

Pc26   MW 30,252   pI 9.57
MKTLAIVTLAVAFCYANAILTNYGTGYGKI
GGVGGLG
HGGYGG
HGGYGG
HGGYGGHGVLAGHGGYGAHGVLAG
HGGYGGHGVLAGHGGYGGHGVLAG
HGGYGGHGILAGHGYGYG
KKGSSSSISSSDLYKHHHGYGT
SSSLSSSDLRRG
LGYGHHGHGYGYG
KSSSSSSSSSSSSSSSSSSSSSSSSSSSS
HYGRGYGHHGHHHGHSSSSISSSDLH
HGLHGYGYKSPTSSISSSDIHYHAKKLLLVTQCIC
GLGRKDVYPATGLGRKDVYPVP
GLGRKDVYPGPGLGRKGVYPGR
GFGVPGPFW

Tyrosinase like protein-1   MW 22,654   pI 8.37
MLFKIALLVLVCVFIIVTGFEDDETDLDKMKIMEEMIKEWKSDNDEIKFTPTQISYLNHLDNRGRGSGRGRGRGNVRGR
GNGQQGRGKGNNRSKRQYEYLPVRKAYRHLSDSERKDFHDAIYQLKHTFSDPTSDLSNYDLFVNLHRSNSAPYAHGG
HAFAGWHRHCLYRFEKALQEINEDVTLCYLDTTMEYNVGR

Fig. 4. Putative secretory gland protein sequences. Underlined sequences indicate signal peptides. Accession numbers: Pc19, JN607210; Pc21, JN607211; Pc22, JN607212; Pc26, JF806320; and tyrosinase-like protein-1, JN607213. Red residues in tyrosinase-like protein-1 indicate conserved sequences in the copper binding sites of tyrosinases.
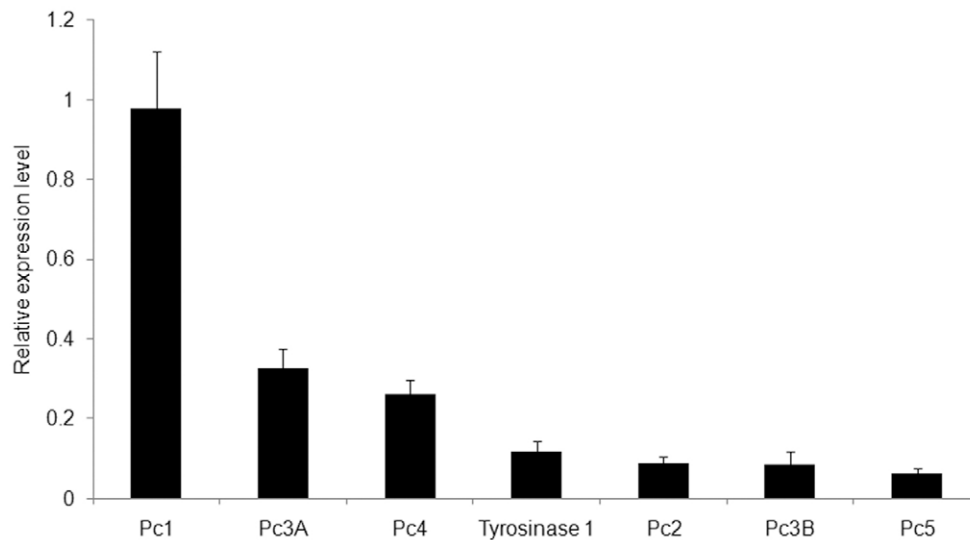
of the Pc1–5 and tyrosinase 1 genes. Control DIG-labeled Pc3A sense RNA showed negligible background staining (Fig. 6A,B). The Pc1 probe strongly labeled the adhesive gland (Fig. 7A) and at higher magnification labeling occurred only in cells producing heterogeneous granules (Fig. 7B). The Pc2 probe hybridized only in cells producing homogeneous granules (Fig. 7C,D). Of the two major Pc3 variants, *in situ* hybridization was carried out only with the RNA of the most abundantly expressed variant, Pc3A, which labeled only those cells producing heterogeneous granules (Fig. 7E,F), consistent with elemental analysis (Wang et al., 2010). The Pc4 probe labeled heterogeneous granule cells. (Fig. 7G,H). The Pc5 probe labeled the adhesive gland unevenly and localized to homogeneous granule-producing cells (Fig. 7I,J). The tyrosinase 1 probe strongly labeled both heterogeneous and homogeneous granule-producing cells throughout the entire adhesive gland. Additionally, tyrosinase 1 labeling in the posterior region of the parathorax parapodia was unambiguous (Fig. 7K,L).
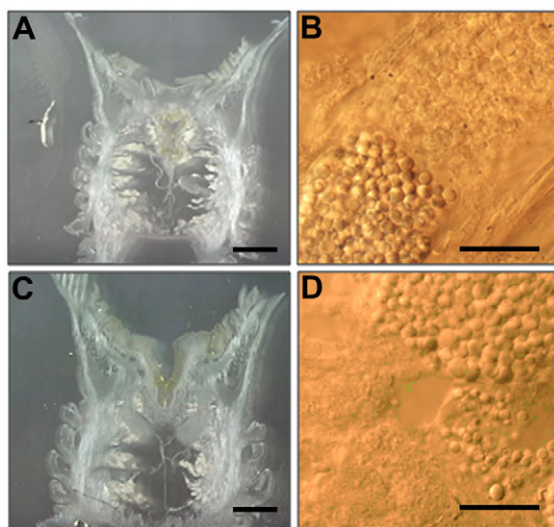

Fig. 6. *In situ* hybridization and immunostaining of negative controls. (A,B) *In situ* hybridization with sense strand Pc3A. (C,D) Immunostaining with anti-digoxigenin. Scale bars: A and C, 100 μm; B and D, 10 μm.

Immunohistochemistry

Antibodies against synthetic peptides predicted to be immunogenic were used to immunolocalize Pc2, Pc4 and Pc5. Highly repetitive, glycine-rich Pc1 did not have a sequence with a predicted high probability of generating an immune response; therefore, raising a peptide antibody to recognize Pc1 was not attempted. The synthetic Pc2, Pc4 and Pc5 peptides generated high-titer antibodies in rabbits. Specificity of the antibodies was verified on western blots with secretory granules isolated from the parathorax (Fig. 8). Anti-Pc2 recognized a pair of bands at ~21 kDa on western blots, consistent with its predicted molecular mass of 21.1 kDa. The anti-phosphoserine antibody recognized a band at ~15 kDa, perhaps corresponding to Pc3A. Anti-Pc4 and anti-Pc5 recognized single bands at ~25 and ~15 kDa bands, consistent with their predicted molecular masses of 24.3 and 14.9 kDa.

The Pc2 antibody produced punctate staining in the adhesive gland (Fig. 9A), which at closer examination localized only in the homogeneous granules (Fig. 9B), consistent with the *in situ* hybridization staining. Phosphorylation of serine is a common modification; therefore, weak staining occurred in much of the tissue with the generic anti-phosphoserine antibody that recognizes Pc3 (Fig. 9C). Nevertheless, close examination of the adhesive gland tissue revealed strong anti-phosphoserine staining of the heterogeneous granules and comparatively little staining of the homogeneous granules (Fig. 9D), consistent with *in situ* hybridization results and elemental mapping. Although it recognized a protein of the expected size on western blots of isolated granules (Fig. 8), anti-Pc4 labeled neither type of granule in tissue cryosections (Fig. 9F). Instead, it labeled the anterior region of the parathorax parapodia and the cells lining the bowtie of tissue below the building organ (Fig. 9E, Fig. 1A). Anti-Pc5 labeled only homogeneous granules (Fig. 9H). Tissue staining controls with anti-DIG as the primary antibody gave negligible background immunostaining (Fig. 6C,D).

A transverse section through the parathorax of a resin-embedded worm was treated with proteinase K, then probed with anti-Pc4. In contrast to cryosections of the adhesive gland (Fig. 9F), heterogeneous granules in the proteolyzed adhesive gland were immunolabeled with anti-Pc4 (Fig. 10A,B). The Pc4 epitope was apparently not accessible in cryosections, but became accessible after protease treatment of resin-embedded tissue. Tyrosinase 1 and Pc4 are both expressed in the first three parapodia. To sub-localize their expression in the
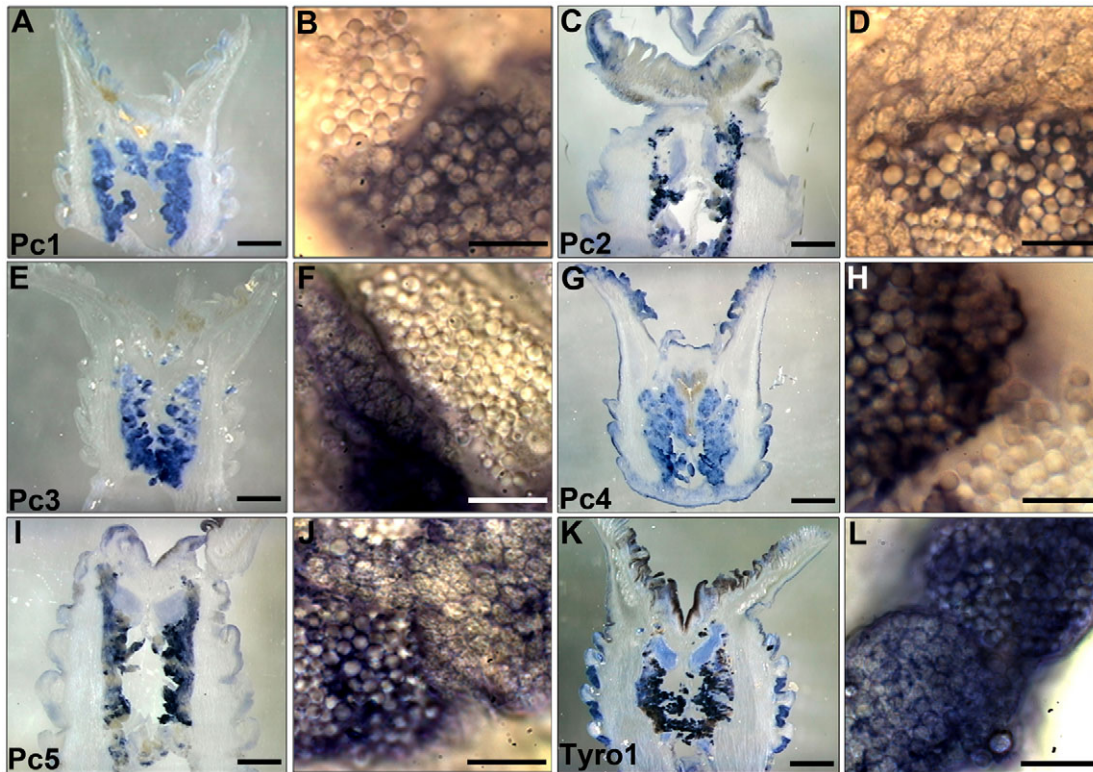
Fig. 7. *In situ* hybridization with highly expressed genes. (A,C,E,G,I,K) Low magnification of coronal cryosections. (B,D,F,H,J,L) Higher magnification of homongeneous and heterogeneous secretory granules. Probes are identified in the lower left of each panel. Scale bars: low magnification panels, 100 µm; high magnification panels, 10 µm.

parapodia, a cryosection was double-labeled with tyrosinase 1–DIG RNA and anti-Pc4 (Fig. 10C). Tyrosinase 1, visualized with an alkaline phosphatase secondary antibody and a blue chromogenic substrate, was expressed in the posterior base of the parathorax parapodia. Pc4, visualized with a far-red fluorescently labeled secondary antibody then false colored green for better contrast, was present in the anterior tips and did not overlap with tyrosinase 1.

Set and cured glue from glass beads that had been bonded by worms during tube reconstruction was recovered for immunolabeling by washing the beads. The glue spots were easily dislodged from the glass beads with 30% acetic acid. The glue was double–labeled with anti-phosphoserine (Pc3), secondarily labeled red, and anti-Pc2, anti-Pc4 or anti-Pc5, secondarily labeled green. The foam structure of the glue was readily apparent in the confocal images (Fig. 11). In several instances, distinct red rings around the pores were apparent inside a more evenly distributed green matrix. The presence of only small areas of yellow demonstrated that the phosphoserine staining (red) and Pc2, Pc4 and Pc5 (green) staining were mostly non-overlapping, and, by inference, the polyanionic and polycationic proteins were poorly mixed.

DISCUSSION
Protein localization
A total of 18 full-length transcripts from a parathorax cDNA library that encode proteins with general characteristics of secreted structural proteins have now been reported, as well as a tyrosinase 1 with a secretion signal peptide. A serine kinase that phosphorylates the polyserines of the Pc3 proteins remains conspicuously absent from the cDNA catalog. Not surprisingly, the most highly expressed structural proteins in healthy adult worms, actively rebuilding tubes, were the first six proteins discovered, either biochemically or through sequencing cDNAs (Fig. 5). The other structural proteins with low relative expression levels may be components of the chitinous cuticle, or chetae, and may be more highly expressed during rapid growth

and/or development. Some time after gluing together the mineral tube the worm lines the interior of the tube with a fabric-like sheath. Little is known about the origin or composition of the sheath; some of the secreted structural proteins may be sheath components.

The localization of the highly expressed proteins is summarized schematically in Fig. 12. On the basis of *in situ* hybridization, polybasic Pc1 and Pc4 were unambiguously co-expressed with
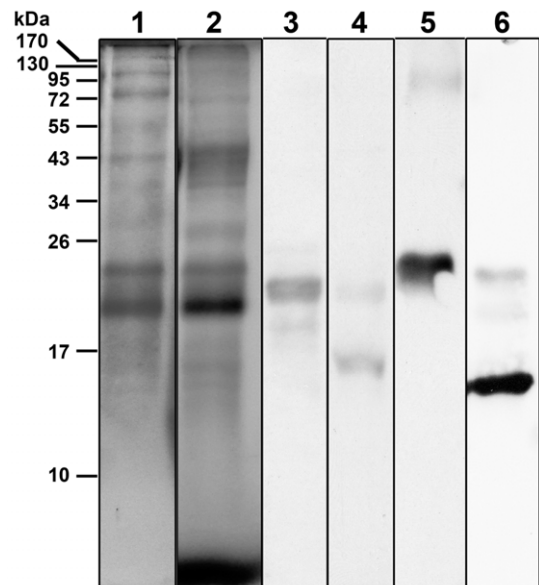

Fig. 8. Gel electrophoresis and western blot analysis of secretory granule proteins. Proteins in granules isolated from the parathorax region were separated by SDS-PAGE. Lanes: 1, Coomassie Blue; 2, NBT stain; 3, anti-Pc2; 4, anti-phosphoserine; 5, anti-Pc4; 6, anti-Pc5.
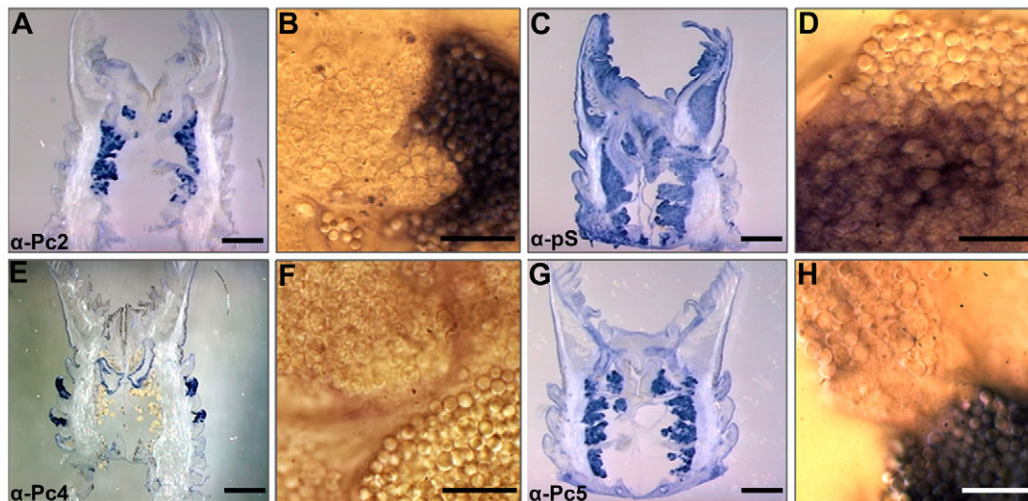
Fig. 9. Immunolabeling of parathorax cryosections. (A,C,E,G) Low magnification of coronal cryosections. (B,D,F,H) Higher magnification of heterogeneous and homogeneous secretory granules in the gland. Scale bars: low magnification panels, 100 µm; higher magnification panels, 10 µm.

polyacidic Pc3A in the cells producing heterogeneous granules. The Pc4 antibody, however, did not recognize either heterogeneous or homogeneous granules in tissue cryosections, although it did label a single band of the expected size on western blots of isolated granules and a region of the first three parapodia in tissue sections, and it convincingly labeled the secreted glue. The epitope was inaccessible in intact tissue secretory granules, but became accessible after denaturation for gel electrophoresis and after protease treatment of the adhesive gland, which localized Pc4 to the heterogeneous granules, consistent with *in situ* hybridization. Exposure of the epitope in the secreted glue may have resulted from the processing of the secreted glue for immunolabeling. The more interesting possibility is that the cryptic epitope was exposed as a result of a structural reorganization concomitant with secretion of the glue. If so, the Pc4 antibody may be a useful probe for glue maturation in future experiments. Its presence in the parapodia suggests Pc4, the fourth most abundantly expressed protein, may be a component of multiple materials secreted by the sandcastle worm. Interestingly, the epitope was not hidden in non-proteolyzed parapodia tissue. Of significance, perhaps, the absence of co-localized NBT staining in the anterior of the thorax parapodia suggests Pc4 does not contain a significant number of dopa residues, at least in the parapodia. Polybasic, histidine-rich Pc2 and Pc5 proteins are both components of the homogeneous granules, as well as the final secreted glue. In short, immunolocalizaton provided definitive evidence for a direct role of Pc2, Pc4 and Pc5 in the formation and structure of the final glue.

The relatively high expression of tyrosinase 1 in heterogeneous and homogeneous granule-producing cells of adults actively synthesizing glue suggests it may have a direct role in the curing, and perhaps even the structure, of the secreted glue. Secreted as a viscous, milky white fluid, the glue turns progressively more reddish brown over several hours, presumably as a result of covalent curing of the glue through quinonic cross-linking. Tyrosinases can catalyze two reactions, the hydroxylation of tyrosines to form dopa, and the further oxidation of dopa to form reactive dopaquinones that undergo Michael addition with nucleophilic sidechains, and other reactions (Sanchez-Ferrer et al., 1995). Covalent cross-linking of the structural dopa proteins may be catalyzed by the tyrosinase, which may be activated during co-secretion. The mussel provides a precedent for such a mechanism. The mussel byssus contains an extractable catechol oxidase activity (Waite, 1985). The mussel enzyme was described as a catechol oxidase because it lacks tyrosine hydroxylase activity. It remains to be determined whether the sandcastle tyrosinase has both oxidase activities. The mussel catechol oxidase is co-packaged in secretory granules with dopa proteins and co-secreted, whereupon it is activated to catalyze dopa-mediated cross-linking (Waite, 1992). The activation trigger for the granular oxidase enzymes, in mussels and sandcastle worms, may be the pH jump that occurs during secretion – from the low pH of secretory granules to the higher external pH – as suggested for other granular enzymes (Johnson et al., 1980; Kelly, 1987). Expression in the parapodia suggests tyrosinase 1, like Pc4, may have multiple functions, perhaps in quinonic tanning of the tube lining. The secreted tyrosinase may be the phenoloxidase activity reported by Vovelle in the sabellarid *Sabellaria aveolata* (Vovelle, 1965).
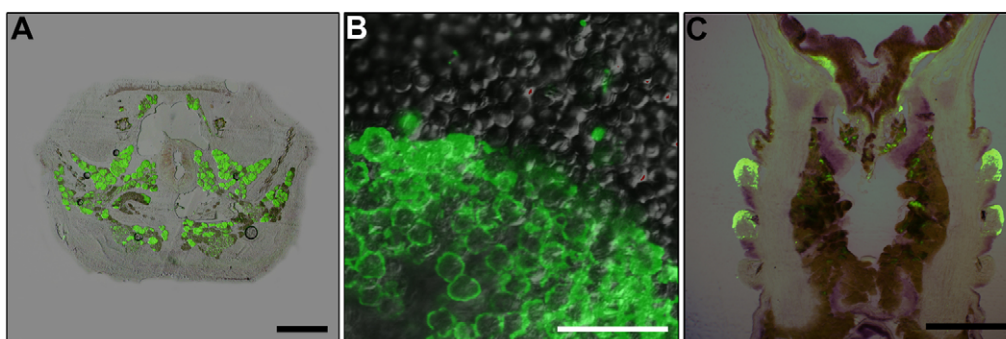

Fig. 10. Localization of Pc4 in proteolyzed tissue. (A) Anti-Pc4 labeling (green) of a resin-embedded transverse section treated with proteinase K. (B) Higher magnification of A. Anti-Pc4 labeled only heterogeneous granules (green). (C) Anti-Pc4 immunolabel (green) overlaid on tyrosinase 1 *in situ* hybridization (purple–dark blue). Scale bars: A and C, 250 µm; B, 10 µm.

Formation of the sandcastle worm glue

The precursors of the sandcastle worm glue are products of the regulated secretory system, which is the secretion pathway for proteins that are released in bursts at rates much faster than protein synthesis. The proteins destined for regulated secretion are concentrated as much as 200-fold during transit from the Golgi apparatus to mature secretory vesicles (Kelly, 1985). The cytoplasm becomes packed with dense secretory vesicles because of their relatively long half-life. It is well known that condensation of proteins into dense secretory granules is, in general, driven by low pH and electrostatic charge neutralization between oppositely charged polyions (Gorr et al., 2005). Mucin, as an example, is an acidic polyanionic glycoprotein condensed into granules through charge shielding by H^+ and divalent Ca^{2+}. Sulfated proteoglycans are polyanionic components of numerous secretory cell types that condense polycationic secreted proteins (Reggio and Dagorn, 1978). In addition to the contribution of low secretory vesicle pH, the requisite condensation of the sandcastle worm glue proteins into the heterogeneous granules could proceed through several electrostatic interactions: polybasic Pc1 and Pc4 may be components of a matrix that neutralize and condense the polyphosphates; or, polyphosphorylated Pc3 may be neutralized and condensed by divalent Mg^{2+} as suggested by colocalization of Mg^{2+} with phosphate exclusively in subgranules; or, as a polyampholyte with acidic and basic domains, Pc3A could self-condense into granules. Of course, more than one of these condensing mechanisms could be operative. What is the counter polyanion that condenses polycationic Pc2 and Pc5 in the homogeneous granules? One possibility is that the secreted glue may contain a significant amount of sulfur (Stewart et al., 2011), the source of which could be an unidentified sulfated proteoglycan that condenses the polybasic proteins.

The final set glue is a solid foam with a mix of open and closed pores, with diameters ranging from less then 1 to greater than $6\,\mu m$ (Stevens et al., 2007). The average pore diameter, $\sim2\,\mu m$, is roughly the same diameter as the homogeneous and heterogeneous granules, but much larger than the polyphosphate/Mg-containing sub-granules. Vovelle reported that the sub-granules swelled after secretion and became the pores of the foamy adhesive mass, while the contents of the homogeneous granules formed a matrix around the pores (Vovelle, 1965). Vovelle's observations are supported by the apparent concentration of polyphosphoserine around the walls of the pores and the non-overlapping distribution of the polybasic proteins observed by immunolocalization (Fig. 11). If the glue was well mixed, as arising from a fluid complex coacervate precursor, the fluorescence would have appeared mostly yellow from the blending of the red and green labels. Instead, for the most part, red and green are distinct with all three antibodies against polybasic proteins. Similarly, the granular components of fresh glue, derived by electrical stimulation of secretion, stained differentially with cationic TB, and also appeared to be poorly mixed (Wang et al., 2010). A caveat is that the polybasic Pc1 protein, highly expressed in heterogeneous granule cells, has not been immunolocalized; therefore, intimate complexation with Pc3A,B in the secreted glue cannot be ruled out.

The detailed mechanisms that cause the granules to swell and aggregate after secretion, turn into a load-bearing glue within $30\,s$ (Stevens et al., 2007), then covalently cure over several hours into a solid foam, are unknown and likely complex. Comparatively well-studied mucin secretion serves as a starting point for discussion. Mucin granules are secreted intact and under normal physiological conditions swell several hundredfold within tens of milliseconds as a result of an influx of water driven by a Donnan potential (Tam
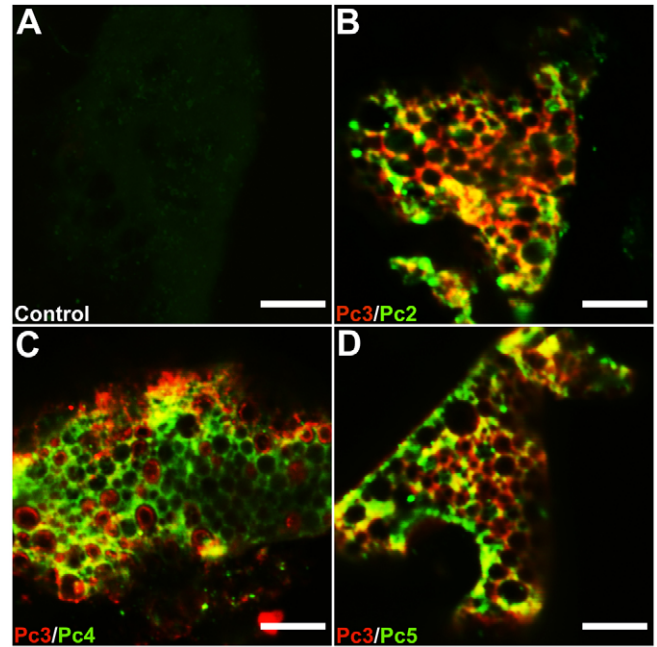

Fig. 11. Glue immunolabeling. (A) Negative controls. (B–D) Double immunolabel with (B) anti-Pc2 (green) and anti-phosphoserine (red), (C) anti-Pc4 (green) and anti-phosphoserine (red), (D) anti-Pc5 (green) and anti-phosphoserine (red). Scale bars: A–D, $20\,\mu m$.

and Verdugo, 1981). The sudden swelling has been described as a critical phenomenon; a 'jack-in-the-box' discontinuous transition from the condensed state to an expanding state – a phase transition unlatched by small changes in environmental conditions (Verdugo, 1991). Accordingly, during mucin exocytosis, exposure to extracellular Na^+ displaces Ca^{2+} in the condensed granules, triggering the transition into small hydrated gels that subsequently anneal into a continuous mass. Similar ion-triggered critical swelling phenomena have been studied in synthetic hydrogels (Tanaka and Fillmore, 1979). For completeness, specific interactions between mucin chains, in addition to Ca^{2+}/H^+ charge shielding, contribute to condensation and expansion (Kesimer et al., 2010).

In broad outline, similar mechanisms may be operative in the swelling and aggregation of the sandcastle worm glue granules. Upon secretion into seawater, the granules are exposed to approximately $0.5\,mol\,l^{-1}$ monovalent Na^+ and Cl^- ions and pH>8, which would have pronounced effects on ionic and electrostatic interactions within the glue. The spike in external ionic strength may disrupt some electrostatic interactions; perhaps between phosphate sidechains and Mg^{2+}, causing the heterogeneous sub-granules to swell as Mg^{2+} is exchanged for Na^+ with an accompanying osmotic influx of water. The nominal pK_a of Pc4 histidines and the nominal second pK_a of Pc3A,B phosphoserines lie between the internal pH of secretory granules (assumed to be low as in other secretory granules) and the elevated pH of seawater, which may effect an increase in the net negative charge of the glue upon secretion that contributes to an influx of Na^+ and water. But none of this explains why heterogeneous sub-granules swell like balloons into polyphosphoserine-lined pores. Further, an influx of water seems counter-productive to formation of a strong glue. Segregation of water, somehow, into the pores of the foam structure may minimize the effects of dilution on cohesive integrity. A solid foam structure may be mechanically and metabolically advantageous (Stewart et al., 2004; Stevens et al., 2007).
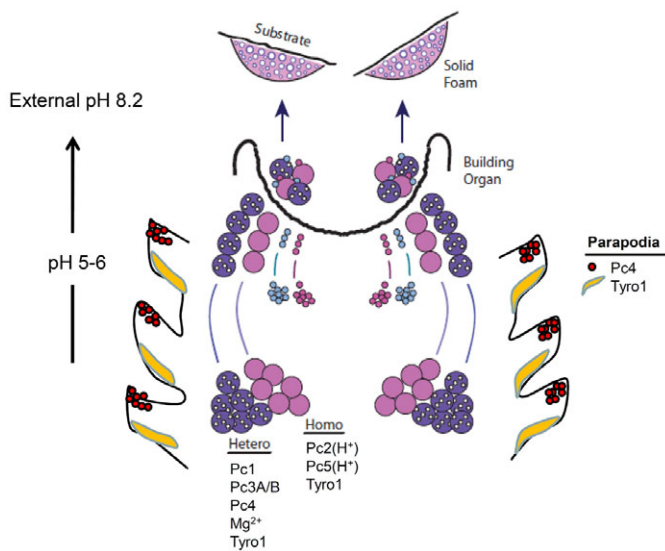
Fig. 12. Summary of adhesive precursor localization.

The rapid setting and slower cure of the secreted glue can proceed through one or more of several speculative pathways. First, associative gelling of the adhesive could occur through electrostatic interactions between the polyphosphates (Pc3A,B) in the heterogeneous granules and the polyamines (Pc2,5) in the homogeneous granules. The worm wiggles newly placed particles as if checking the set before letting go (Stevens et al., 2007). This process could physically facilitate partial mixing of the granule contents and initial gellation. Second, Mg^{2+} and polyphosphate are soluble at low pH but insoluble at pH 8.2 in $450\,mmol\,l^{-1}$ NaCl (Stewart et al., 2010). Transition of Pc3A,B from a gel-like state to an insoluble complex would harden the initially fluid glue, though this mechanism seems contradictory to swelling induced by Mg^{2+}/Na^{+} exchange. Third, the secreted glue contains significant quantities of transition metals, including Fe, Mn, Zn and Cu (Stewart et al., 2011). Fe is concentrated 10^{5}-fold in the glue relative to seawater; the others are concentrated 10^{3}- to 10^{4}-fold. Formation of intermolecular histidine–transition metal coordination complexes, as the imidazolyl sidechains are deprotonated by the pH increase upon secretion, would provide rapid pH-triggered cohesive integrity. There is also potential for the formation of tris-dopa–Fe(III) coordination complexes, as demonstrated in the mussel adhesive plaque proteins (Harrington et al., 2010; Wilker, 2010; Zeng et al., 2010). The Fe to dopa molar ratio in the sandcastle worm glue was estimated to be between 1:5 and 1:10 (Stewart et al., 2011). Fourth, as discussed earlier, the co-secreted tyrosinase could catalyze quinonic cross-linking during secretion. Both heterogeneous and homogeneous granules are fluorescent while still in the secretory cells of the adhesive gland. One source of this fluorescence could be quinone cross-links, which suggests the adhesive proteins may be partially cross-linked before secretion.

CONCLUSIONS

The glue with which sandcastle worms build composite mineralized tubes consists of oppositely charged polyelectrolytes, distinguished by extremely phosphorylated proteins and a set of polyamino proteins. The components are separately packaged into at least four co-secreted parts, though the complete significance of the pre-secretion separation remains obscure. The involvement of polyelectrolytes and electrostatic interactions may be a general theme in natural underwater

bioadhesives. In addition to the sandcastle worm glue, several other natural bioadhesive examples suggest phosphatidyl side-chains may contribute specific and advantageous functionalities to underwater adhesives; functionalities that include ionic strength-independent interfacial adhesion, formation of electrostatic complexes with polyamines, formation of coordination complexes with metal ions, and pH-dependent solubility with divalent Ca^{2+}/Mg^{2+} (Stewart et al., 2011). The greatest advantage, compared with other acidic functional groups, may be a nominal pK_{a2} close to neutral pH, which allows the chemical functionality of peptidyl phosphates to be modulated by small, near-physiological pH changes. Covalent curing of the sandcastle worm glue subsequent to secretion may be catalyzed by a co-secreted tyrosinase. As a final point, the regulated secretory system, in numerous cases based on electrostatic condensation of polyions, may have been a pre-adaptation upon which bioadhesives based on oppositely charged polyelectrolytes evolved. Correlatively, the requirement for intracellular condensation of secreted proteins may have restricted the composition of underwater bioadhesives secreted *via* the regulated pathway to paired oppositely charged polyelectrolytes, a general observation that may inform characterization of other natural underwater adhesives. The identification and localization of the sandcastle worm glue components mark a path for detailed experiments to sort through the potential mechanisms of sandcastle worm glue formation and curing in the first few 10s of seconds after secretion.

REFERENCES

Bergeron, J. A. and Singer, M. (1958). Metachromasy: an experimental and theoretical reevaluation. *J. Biophys. Biochem. Cytol.* **4**, 433-457.

Case, S. T., Powers, J., Hamilton, R., Burton, M. J. (1994). Silk and silk proteins from two aquatic insects. In *ACS Symposium Series*, Vol. 544. Washington, DC: American Chemical Society.

Endrizzi, B. J. and Stewart, R. J. (2009). Glueomics: an expression survey of the adhesive gland of the sandcastle worm. *J. Adhes.* **85**, 546-559.

Fewkes, J. W. (1889). New Invertebrata from the coast of California. *Bull. Essex Inst.* **21**, 99-147.

Flammang, P., Lambert, A., Bailly, P. and Hennebert, E. (2009). Polyphosphoprotein-containing marine adhesives. *J. Adhes.* **85**, 447-464.

Galler, R., Rydlander, L., Riedel, N., Kluding, H. and Edstrom, J. E. (1984). Balbiani ring induction in phosphate metabolism. *Proc. Natl. Acad. Sci. USA* **81**, 1448-1452.

Gorr, S. U., Venkatesh, S. G. and Darling, D. S. (2005). Parotid secretory granules: crossroads of secretory pathways and protein storage. *J. Dent. Res.* **84**, 500-509.

Harrington, M. J., Masic, A., Holten-Andersen, N., Waite, J. H. and Fratzl, P. (2010). Iron-clad fibers: a metal-based biological strategy for hard flexible coatings. *Science* **328**, 216-220.

Jensen, R. A. and Morse, D. E. (1988). The bioadhesive of *Phragmatopoma californica* tubes: a silk-like cement containing L-DOPA. *J. Comp. Physiol. B* **158**, 317-324.

Johnson, R. G., Carty, S. E., Fingerhood, B. J. and Scarpa, A. (1980). The internal pH of mast cell granules. *FEBS Lett.* **120**, 75-79.

Kelly, R. B. (1985). Pathways of protein secretion in eukaryotes. *Science* **230**, 25-32.

Kelly, R. B. (1987). Protein transport. From organelle to organelle. *Nature* **326**, 14-15.

Kesimer, M., Makhov, A. M., Griffith, J. D., Verdugo, P. and Sheehan, J. K. (2010). Unpacking a gel-forming mucin: a view of MUC5B organization after granular release. *Am. J. Physiol. Lung Cell Mol. Physiol.* **298**, L15-L22.

Lee, B. P., Messersmith, P. B., Israelachvili, J. N. and Waite, J. H. (2011). Mussel-inspired adhesives and coatings. *Annu. Rev. Mater. Res.* **41**, 99-132.

Paz, M. A., Fluckinger, R., Boak, A., Kagan, H. M. and Gallop, P. M. (1991). Specific detection of quinoproteins by redox-cycling staining. *J. Biol. Chem.* **266**, 689-692.

Reggio, H. and Dagorn, J. C. (1978). Ionic interactions between bovine chymotrypsinogen A and chondroitin sulfate: a possible model for molecular aggregation in zymogen granules. *J. Cell Biol.* **78**, 951-957.

Rozen, S. and Skaletsky, H. J. (2000). Primer3 on the WWW for general users and for biologist programmers. In *Bioinformatics Methods and Protocols: Methods in Molecular Biology* (ed. S. Krawetz and S. Misener), pp. 365-386. Totowa, NJ: Humana Press.

Sanchez-Ferrer, A., Rodriguez-Lopez, J. N., Garcia-Canovas, F. and Garcia-Carmona, F. (1995). Tyrosinase: a comprehensive review of its mechanism. *Biochim. Biophys. Acta* **1247**, 1-11.

Shao, H., Bachus, K. N. and Stewart, R. J. (2009). A water-borne adhesive modeled after the sandcastle glue of *P. californica. Macromol. Biosci.* **9**, 464-471.

Stevens, M. J., Steren, R. E., Hlady, V. and Stewart, R. J. (2007). Multiscale structure of the underwater adhesive of *Phragmatopoma californica*: a nanostructured latex with a steep microporosity gradient. *Langmuir* **23**, 5045-5049.

Stewart, R. J. and Wang, C. S. (2010). Adaptation of caddisfly larval silks to aquatic habitats by phosphorylation of h-fibroin serines. *Biomacromolecules* **11**, 969-974.

Stewart, R. J., Weaver, J. C., Morse, D. E. and Waite, J. H. (2004). The tube cement of *Phragmatopoma californica*: a solid foam. *J. Exp. Biol.* **207**, 4727-4734.

Stewart, R. J., Wang, C. S. and Shao, H. (2010). Complex coacervates as a foundation for synthetic underwater adhesives. *Adv. Colloid. Interface. Sci.* **167**, 85-93.

Stewart, R. J., Ransom, T. C. and Hlady, V. (2011). Natural underwater adhesives. *J. Polym. Sci. Pol. Phys.* **49**, 757-771.

Tam, P. Y. and Verdugo, P. (1981). Control of mucus hydration as a Donnan equilibrium process. *Nature* **292**, 340-342.

Tanaka, T. and Fillmore, D. J. (1979). Kinetics of swelling of gels. *J. Chem. Phys.* **70**, 1214-1218.

Verdugo, P. (1991). Mucin exocytosis. *Am. Rev. Respir. Dis.* **144**, S33-S37.

Vovelle, J. (1965). Le tube de *Sabellaria alveolata* (L.) Annelide Polychete Hermellidae et son ciment. Etude ecologique, experimentale, histologique et histochimique. *Arch. Zool. Exp. Gen.* **106**, 1-187.

Waite, J. H. (1985). Catechol oxidase in the byssus of the common mussel, *Mytilus edulis* L. *J. Mar. Biol. Assoc. UK* **65**, 359-371.

Waite, J. H. (1992). The formation of mussel byssus: anatomy of a natural manufacturing process. *Results Probl. Cell Differ.* **19**, 27-54.

Waite, J. H., Jensen, R. A. and Morse, D. E. (1992). Cement precursor proteins of the reef-building polychaete *Phragmatopoma californica* (Fewkes). *Biochemistry* **31**, 5733-5738.

Waite, J. H., Andersen, N. H., Jewhurst, S. and Sun, C. (2005). Mussel adhesion: finding the tricks worth mimicking. *J. Adhes.* **81**, 297-317.

Wang, C. S., Svendsen, K. K. and Stewart, R. J. (2010). Morphology of the adhesive system in the sandcastle worm, *Phragmatopoma californica*. In *Biological Adhesive Systems: From Nature to Technical and Medical Applications* (ed. J. von Byern and I. Grunwald). New York: Springer.

Wilker, J. J. (2010). Marine bioinorganic materials: mussels pumping iron. *Curr. Opin. Chem. Biol.* **14**, 276-283.

Winslow, B. D., Shao, H., Stewart, R. J. and Tresco, P. A. (2010). Biocompatibility of adhesive complex coacervates modeled after the sandcastle glue of *Phragmatopoma californica* for craniofacial reconstruction. *Biomaterials* **31**, 9373-9381.

Yonemura, N., Sehnal, F., Mita, K. and Tamura, T. (2006). Protein composition of silk filaments spun under water by caddisfly larvae. *Biomacromolecules* **7**, 3370-3378.

Zeng, H., Hwang, D. S., Israelachvili, J. N. and Waite, J. H. (2010). Strong reversible Fe^{3+}-mediated bridging between dopa-containing protein films in water. *Proc. Natl. Acad. Sci. USA* **107**, 12850-12853.

Zhao, H., Sun, C., Stewart, R. J. and Waite, J. H. (2005). Cement proteins of the tube-building polychaete *Phragmatopoma californica. J. Biol. Chem.* **280**, 42938-42944.